Role of Cofilin in Epidermal Growth Factor–stimulated Actin Polymerization and Lamellipod Protrusion

Amanda Y. Chan,* Maryse Bailly,* Noureddine Zebda, Jeffrey E. Segall, and John S. Condeelis

Department of Anatomy and Structural Biology, Albert Einstein College of Medicine, Bronx, New York 10461

Abstract. Stimulation of metastatic MTLn3 cells with epidermal growth factor (EGF) causes a rapid and transient increase in actin nucleation activity resulting from the appearance of free barbed ends at the extreme leading edge of extending lamellipods. To investigate the role of cofilin in EGF-stimulated actin polymerization and lamellipod extension in MTLn3 cells, we examined in detail the temporal and spatial distribution of cofilin relative to free barbed ends and characterized the actin dynamics by measuring the changes in the number of actin filaments. EGF stimulation triggers a transient increase in cofilin in the leading edge near the membrane, which is precisely cotemporal with the appearance of free barbed ends there. A deoxyribonuclease I binding assay shows that the number of filaments per cell increases by 1.5-fold after EGF stimulation. Detection of pointed ends in situ using deoxyribonuclease I binding demonstrates that this increase in the number of pointed ends is confined to the leading edge compartment, and does not occur within stress fibers or in the general cytoplasm. Using a light microscope severing assay, cofilin's severing activity was observed directly in cell extracts and shown to be activated after stimulation of the cells with EGF. Microinjection of function-blocking antibodies against cofilin inhibits the appearance of free barbed ends at the leading edge and lamellipod protrusion after EGF stimulation. These results support a model in which EGF stimulation recruits cofilin to the leading edge where its severing activity is activated, leading to the generation of short actin filaments with free barbed ends that participate in the nucleation of actin polymerization.

Key words: metastasis • chemotaxis • F-actin severing • motility • actin-related protein (ARP) 2/3

Introduction

Cell motility plays an important role in many basic biological processes, including embryogenesis, neurite growth, wound healing, inflammation, and cancer metastasis. Motility of crawling cells is dependent on the ability to extend F-actin–rich protrusions, usually in the form of lamellipods (Abercrombie et al., 1970; Chen et al., 1994; Verschueren et al., 1994; Xie et al., 1995). Protrusion of such actin-rich lamellipods in moving cells requires cycles of actin polymerization and depolymerization (actin polymerization transients) (Lauffenburger and Horwitz, 1996; Mitchison and Cramer, 1996; Bailly et al., 1998a; Condeelis, 1998).

Previous studies have demonstrated the requirement for free barbed ends in the control of this cycle (Handel et al., 1990; Symons and Mitchison, 1991; Chan et al., 1998). We have shown previously that stimulation of metastatic MTLn3 cells with EGF causes a transient increase in actin nucleation activity resulting from the appearance of free barbed ends at the extreme leading edge of extending lamellipods (Chan et al., 1998). This increase in actin nucleation activity is associated with an increase in the number of filaments throughout the leading edge (Bailly et al., 1999; Chan et al., 1998). Coincident with the increase in barbed and pointed ends, a general decrease in filament length with a specific loss of long filaments is observed at the leading edge of EGF-stimulated MTLn3 cells (Bailly et al., 1999).

The molecular mechanism(s) for the appearance of free barbed ends at the leading edge is still unclear. The currently popular models propose that free barbed ends arise by either (A) uncapping of barbed ends, (B) severing of noncovalent bonds in F-actin to produce short filaments with free barbed ends, or (C) de novo nucleation of filaments from a nucleation template.

There is evidence both for and against model A. Studies

in platelets suggest that uncapping of barbed ends by capping protein could be a major mechanism for the production of free barbed ends in response to thrombin stimulation (Hartwig et al., 1995). However, similar studies in *Dictyostelium* rule out uncapping by capping protein as a mechanism for the production of free barbed ends during chemotactic stimulation (Eddy et al., 1997). Furthermore, the increase in barbed end number after stimulation of tumor cells with EGF is accompanied by the shortening of actin filaments (Bailly et al., 1999), which is inconsistent with an uncapping mechanism. In support of models B and C, the decrease in filament length that accompanies the increase in filament number after EGF stimulation suggests that either a severing activity is switched on at the leading edge, resulting in the generation of short filaments with free barbed and pointed ends, or that de novo nucleation from a template like the actin-related protein (Arp)[1] 2/3 complex has occurred, resulting in the appearance of free barbed ends. In vitro studies have shown that cofilin increases the number of free barbed ends by severing filaments, thereby increasing the rate of actin polymerization (Du and Freiden, 1998; Maciver et al., 1998; Ichetovkin et al., 2000). Model C has received more attention recently with the discovery of the Arp2/3 complex and its ability to nucleate actin polymerization through regulation by members of the Wiskott-Aldrich syndrome protein (WASP) family of proteins (Mullins et al., 1998; Egile et al., 1999; Machesky et al., 1999; Rohatgi et al., 1999; Welch, 1999).

The ADF/cofilin (cofilin) family of proteins is capable of binding to both G- and F-actin to increase the rate of depolymerization of actin filaments (for review see Bamburg, 1999; Bamburg et al., 1999). The mechanism(s) by which depolymerization is enhanced involves both filament severing to increase the number of depolymerizing ends (Du and Freiden, 1998; Maciver et al., 1998; Ichetovkin et al., 2000), and a cofilin-induced increase in the off-rate from the pointed ends (Carlier et al., 1997), potentially through a change in the twist in the actin filaments (McGough et al., 1997; Bamburg, 1999; Bamburg et al., 1999). Cofilin can also increase the number of free barbed ends by severing filaments, thereby increasing the rate of actin polymerization (Du and Freiden, 1998; Maciver et al., 1998; Ichetovkin et al., 2000). Hence, cofilin is capable of increasing the rate of actin polymerization, depolymerization, and the number of barbed ends in vitro. Translocation of cofilin to the plasma membrane where barbed ends appear after stimulation has been shown in studies using HL-60 cells (Suzuki et al., 1995), neutrophils (Djafarzadeh and Niggli, 1997; Heyworth et al., 1997), and in flattened *Dictyostelium* under starvation stress (Aizawa et al., 1995), suggesting that cofilin may participate in barbed end mobilization at the membrane.

To investigate the role of cofilin in EGF-stimulated actin polymerization in MTLn3 cells, we examined in detail the temporal and spatial distribution of cofilin relative to free barbed ends, and characterized the actin dynamics by measuring changes in the number of filaments using two different techniques. We used a light microscope severing assay to determine if cofilin severing activity is turned on during EGF stimulation of MTLn3 cells. Furthermore,

---
[1]*Abbreviation used in this paper:* Arp, actin-related protein.

function-blocking antibodies that inhibit cofilin's severing activity were used to assess the role of cofilin in vivo. Our results indicate that cofilin plays a direct role in the mobilization of barbed ends in the leading edge and is necessary for the protrusion of lamellipods in response to EGF stimulation.

Materials and Methods

Cell Culture

MTLn3 cells were grown in α-MEM (Gibco Laboratories) supplemented with 5% FCS, as described previously (Segall et al., 1996; Bailly et al., 1998b).

Preparation of Cofilin Antibodies

Inhibitory (Ab286) and noninhibitory (Ab287) antibodies were generated against rat cofilin peptides containing amino acids 104–117 and 57–71, respectively. Based on comparison with the atomic structure of cofilin (Fedorov et al., 1997), the peptide 104–117 (WAPESAPLKSKMIY) contains the sequence identified as both the actin-binding and phosphatidylinositol 4,5-bisphosphate (PIP2)-binding site on cofilin (Yonezawa et al., 1991). Antibodies generated against this sequence should block the interaction between cofilin and actin. On the other hand, the peptide 57–71 (VGD-VGQTVDDAYTTF) is not at the actin–cofilin interface, and thus represented a candidate sequence for production of an antibody (Ab287) that would not block the interaction between actin and cofilin. The peptides were synthesized as a multiple antigen peptide system (MAPS) (Posnett et al., 1988; Posnett and Tam, 1989) containing four branches, and injected into rabbits without further coupling (Covance). Immunoreactive sera were subsequently affinity purified on the same peptides immobilized on Sepharose matrices.

Specificity of cofilin antibodies was assessed by Western blot (Ab287) and immunoprecipitation analysis (Ab286, Ab287) using MTLn3 cell lysates and purified recombinant rat cofilin as a positive control. The antibody Ab287 recognizes a single polypeptide of 21 kD in Western blots of MTLn3 cell lysates and purified rat cofilin. In addition, both antibodies (Ab286, Ab287) precipitate from whole cell homogenates of MTLn3 cells a single 21-kD polypeptide that binds anticofilin (data not shown).

Cofilin Immunofluorescence

MTLn3 cells were plated on Mattek dishes as described previously (Chan et al., 1998), serum starved for 3 h in α-MEM supplemented with 0.35% BSA and 12 mM Hepes, pH 7.5 (starvation medium), and stimulated with a final concentration of 5 nM EGF in starvation medium, or left untreated. Cells were fixed with 3.0% formaldehyde, 0.1% (vol/vol) glutaraldehyde, and 0.02% NaN$_3$ in PBS, pH 7.35, (145 mM NaCl, 4 mM NaH$_2$PO$_4$, 6 mM Na$_2$HPO$_4$) for 1 h, washed four times in PBS, and permeabilized with 0.5% Triton X-100 in PBS for 15 min. They were then washed three times in PBS, once in TBS (20 mM Tris, 154 mM NaCl, pH 8), and rinsed twice with NaBH$_4$ in TBS for 15 min to reduce glutaraldehyde autofluorescence. The preparations were then washed four times, and blocked and stabilized by incubation for 20 min with 5 μM unlabeled phalloidin (Sigma Chemical Co.) in TBS supplemented with 1% BSA and 1% FCS. Cells were further incubated with anticofilin antibodies (Ab287, 5 μg/ml), followed by FITC-conjugated anti–rabbit antibodies (Cappel Laboratories), and mounted as described previously (Bailly et al., 1999). For F-actin visualization in the same cells, 0.5 μM rhodamine-labeled phalloidin (Molecular Probes) was used during the blocking step.

Visualization of Free Barbed Ends

Nucleation sites (barbed ends) were localized using a previously described protocol (Chan et al. 1998; Bailly et al., 1999) with slight modifications. In brief, the cells were permeabilized for 1 min in presence of 0.45 μM of G-actin (either rhodamine-labeled or biotin-labeled) in buffer C (138 mM KCl, 10 mM Pipes, 0.1 mM ATP, 3 mM EGTA, 4 mM MgCl$_2$, pH 6.9) with 1% BSA and 0.025% saponin. After fixation and subsequent washes, rhodamine-actin incorporation was visualized directly on the fluorescence microscope, while biotin-actin distribution was identified using Cy3-coupled antibiotin antibodies (Sigma Chemical Co.). Previous work has shown

that both techniques gave similar results in terms of localization and quantitation of free barbed ends (Bailly et al., 1999).

Quantitation of Free Pointed Ends

The number of free pointed ends was determined using the DNase I inhibition assay as described previously (Podolski and Steck, 1990; Eddy et al., 1997). In brief, MTLn3 cells were starved for 3 h and detached from plates (Chan et al., 1998), and concentrated to 2×10^7 cells/ml in starvation buffer. At various times after stimulation, the cells were lysed by adding an equal volume of L buffer (10 mM imidazole-acetate, 3.3 mM Tris-acetate, pH 7.5, 50 mM KCl, 2.2 mM Mg-acetate, 4 mM EGTA, 0.55 mg/ml BSA, 0.5 mM ATP, 1 μg/ml each of leupeptin, pepstatin, and chymostatin, 0.25% Triton X-100, and 20 μM phalloidin). Lysates were vortexed for 2 s and immediately microfuged at 4°C for 1 min at 8,700 g. The low-speed Triton-insoluble cytoskeletal pellet was resuspended on ice in 10% lysate volume of L buffer and incubated at 37°C for 30 min to polymerize all residual G-actin into the cytoskeleton. The sample was diluted to 3.33×10^6 cell equivalents/ml in L buffer and incubated with 8.8 nM DNase I for 17 min at room temperature. [^{3}H]DNA (0.011 μg/μl) was then added to the mixture for another 17 min. The reaction was terminated and unhydrolyzed DNA was precipitated by the addition of ice-cold 10% TCA; the radioactivity in the supernatant was analyzed. The number of filament pointed ends was calculated by fitting experimental cpm values to a rabbit G-actin standard curve at a fixed DNase I concentration.

Visualization of Free Pointed Ends

Although DNase I can be used for the staining of either G- or F-actin, the specificity of DNase I staining is determined by the buffer conditions. For staining of G-actin, the G-actin pool has to be stabilized first by 10% ice-cold glycerol and MgCl₂ before application of DNase I (Knowles and McCulloch, 1992). In our study, we used DNase I to stain the pointed ends of F-actin. Thus, the cells were permeabilized in a glycerol-free saponin extraction buffer, and washed extensively in an F-actin stabilization buffer to remove all traces of G-actin before the application of DNase I. The F-actin pool was selectively stabilized by 20 μM phalloidin and 0.5 μM cytochalasin D to prevent depolymerization.

Pointed ends were visualized using immunofluorescence with antibodies against DNase I to detect incorporation of exogenous DNase I in permeabilized MTLn3 cells. In brief, MTLn3 cells grown on Mattek dishes were starved for 3 h in starvation buffer, stimulated with EGF, and permeabilized for 30 s with buffer B (5 mM KCl, 137 mM NaCl, 4 mM NaHCO₃, 0.4 mM KH₂PO₄, 1.1 mM Na₂HPO₄, 2 mM MgCl₂, 5 mM Pipes, and 5.5 mM glucose, pH 7.2) containing 0.025% saponin, 20 μM phalloidin, and 4 mM EGTA. After washes with buffer B containing 20 μM phalloidin and 4 mM EGTA to remove all G-actin, cells were incubated with 1 μM DNase I (diluted in 10 mM imidazole-acetate, pH 7.5, 3.25 mM Tris-acetate, 51 mM KCl, 2.24 mM Mg-acetate, 0.54 mM BSA, and 4.93 mM Mn-acetate) and 0.5 μM cytochalasin D for 17 min. After a brief wash with buffer B containing 20 μM phalloidin and 4 mM EGTA to remove DNase I not bound to the actin cytoskeleton, cells were fixed with 3.7% formaldehyde in buffer B for 5 min, followed by a 10-min incubation with 0.1 M glycine in buffer B. Further steps were carried out as described for cofilin immunofluorescence.

Direct Observation of Actin Filament Severing by MTLn3 Cell Lysates

The severing of actin filaments by cell lysates prepared from MTLn3 cells was observed microscopically in a flow cell coated with 0.2% nitrocellulose in amylacetate. After a 1-h incubation with nitrocellulose, antibiotin antibodies diluted in ISAP buffer (20 mM Tris-HCl, pH 7.5, 5 mM EGTA, 2 mM MgCl₂, 50 mM KCl, 1 mM ATP, 1 mM DTT) were perfused into the chamber for 5 min. The remaining binding sites were blocked with ISAP buffer containing 0.5 mg/ml BSA. Rhodamine and biotin-labeled F-actin were prepared by incubating 0.4 μM rhodamine-labeled actin, 0.2 μM biotin-labeled actin, and 1.4 μM unlabeled actin in ISAP buffer and 0.2 μM phalloidin for no more than 1.5 h. The flow cell was filled with 0.04 μM rhodamine/biotin-labeled F-actin in antibleaching buffer (ISAP buffer containing 5 mg/ml BSA, 0.036 mg/ml catalase, 0.02 mg/ml glucose oxidase, 6 mg/ml glucose, 100 mM DTT, 1 mM ATP) for 5 min. Unbound F-actin was washed away with antibleaching buffer and severing was initiated by replacement of the flow cell solution with cell lysate prepared as described below.

MTLn3 cell lysates were prepared by lysing one part of cell suspension (8×10^6 cells/ml) in 12 parts of lysis buffer (20 mM Tris-HCl, pH 7.5, 5 mM EGTA, 0.5 mM MgCl₂, 0.5% Triton X-100, 0.5 mM ATP, 5 mg/ml BSA, 0.036 mg/ml catalase, 0.02 mg/ml glucose oxidase, 6 mg/ml glucose, 100 mM DTT, and protease inhibitors) at the times indicated after stimulation of cells with EGF. For antibody experiments, cell lysates were incubated with a molar excess of anticofilin or nonimmune IgG for 1 h on ice. The relative number of filaments was calculated as the ratio of the number of filaments at 20 min divided by the number of filaments 30 s after perfusion in the same field. The first measurement was made after perfusion so that filament breakage caused by perfusion would not be scored. Filament breakage was never observed due to perfusion of lysis buffer alone.

Microinjection

Cells were grown on Mattek dishes as described above and placed in L15 medium (Life Technologies) with 0.35% BSA for 1–2 h before injection. Microinjection was conducted using an Eppendorf semiautomated microinjection system using needles pulled on a Sutter p87 micropipette puller. Antibodies (nonimmune rabbit IgG or Ab286 anticofilin at 6 mg/ml in PBS) were mixed with FITC-labeled dextran (0.5–1 mg/ml final concentration; Molecular Probes). Cells were allowed to recover for 1–2 h before further manipulations. For time lapse video microscopy, injected cells were identified directly using the FITC fluorescence of the injected dextran. For F-actin quantitation and barbed end localization, the injected cells were further localized after fixation using FITC-conjugated anti–rabbit antibodies (Cappel Laboratories). From the settings used for microinjection, we estimated a volume of injection ranging between 1 and 10% of the total cell volume, based on calibration of this microinjection system as reported elsewhere (Minaschek et al., 1989). This would deliver between 0.8 and 8 μM of anticofilin Fab binding sites per cell. Since the concentration of cofilin in MTLn3 cells is 6.0 ± 0.5 μM (data not shown), we calculated that under these conditions, the microinjection delivered between 0.13 and 1.33 anticofilin Fab binding sites per molecule of cofilin.

Measurement of Lamellipod Extension

Protrusive activity after EGF stimulation was recorded using time lapse video microscopy and quantified as an increase in total cell area as described previously (Segall et al., 1996; Bailly et al., 1998b).

Fluorescence Quantification

Images were taken using constant settings on an Olympus I ×70 microscope with 60× NA 1.4 infinity-corrected optics coupled to a computer-driven cooled CCD camera using IPLab Spectrum software (Vaytek). The digitized images were converted linearly in NIH Image and analyzed using a program described previously (Bailly et al., 1999). Fluorescence in the cell cortex due to cofilin, rhodamine-actin, or DNase I staining was expressed as the mean pixel intensity within 1.1 μm of the cell membrane and covering the whole cell perimeter. The intensity of DNase I staining in stress fibers was quantitated as relative pixel intensity in random spots along stress fibers. The percentage of cofilin at the leading edge was calculated as the intensity of cofilin at the leading edge divided by the total cofilin intensity of the whole cell.

For F-actin quantification, the relative amounts of F-actin present in the cells were evaluated using rhodamine-phalloidin (Molecular Probes) staining as described previously (Bailly et al., 1999). Quantitation of fluorescence intensity was done as described above, using a derivative of the same program to obtain the cell area and the mean intensity of the whole cell.

Results

Spatial and Temporal Distribution of Cofilin in MTLn3 Cells

To study the relationship between cofilin and the appearance of free barbed ends during stimulated cell motility, the distribution of cofilin in MTLn3 cells was examined at various times after EGF stimulation. To localize free barbed ends, cells were permeabilized in detergent containing rhodamine-actin at concentrations sufficient to
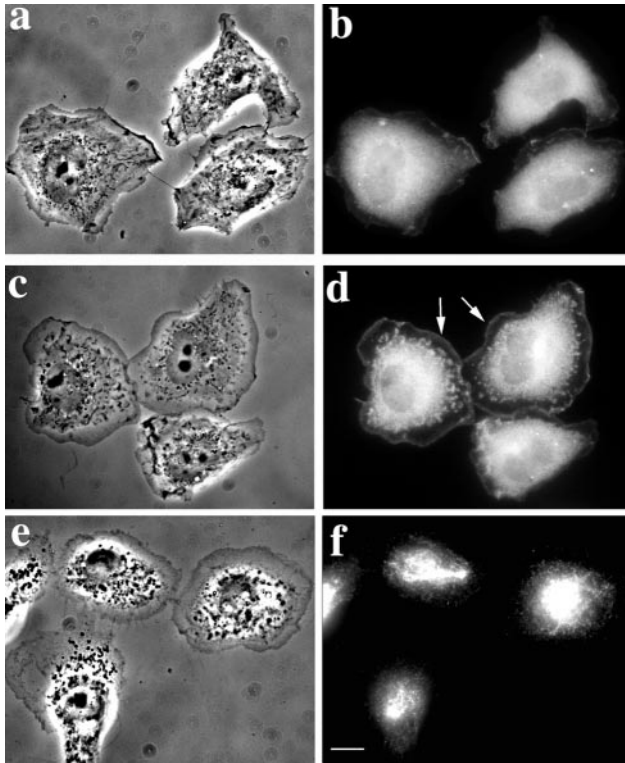
Figure 1. Cofilin is recruited to the leading edge after EGF stimulation. MTLn3 cells either unstimulated (a and b) or stimulated with EGF for 50 s (c–f) were fixed and permeabilized (a–d), or permeabilized then fixed (e and f), and immunostained for cofilin using anticofilin Ab287. In unstimulated cells, cofilin is distributed diffusely in the cytoplasm. Upon EGF stimulation, cofilin is recruited to the leading edge (arrows), which is circumferential in cells stimulated uniformly with EGF. Permeabilization with saponin before fixation resulted in the loss of cofilin from cells, especially at the leading edge (f). Bar, 10 μm.

Figure 3. Cofilin is present in the leading edge after EGF stimulation at the time of appearance of barbed ends. Cells were stimulated for 50 s with EGF. The distribution of rhodamine-actin (i.e., barbed ends, filled squares) and cofilin (open symbols) was measured as a function of distance from the tip of the lamellipod. Cofilin fluorescence was measured both in fixed then permeabilized (open squares), and permeabilized and then fixed (open circles) cells. Cofilin fluorescence at the leading edge decreases dramatically in cells permeabilized before fixation. Membrane, plasma membrane at the tip of the lamellipod. Base, backmost boundary of the lamellipod that was the original edge of the cell before lamellipod extension.

support only barbed end polymerization (Chan et al., 1998). However, under these conditions, we found that permeabilization before fixation extracted cofilin from the leading edge. The extent of this extraction is shown in Fig. 1, e and f (see also Fig. 3). To preserve the cofilin distribution in MTLn3 cells, it was necessary to fix cells with a
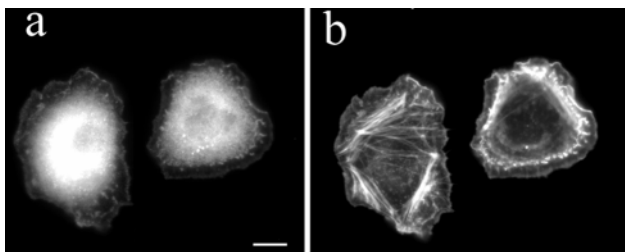

Figure 2. Cofilin colocalizes with F-actin at the leading edge after stimulation. Cofilin was localized by immunostaining with Ab287 in cells stimulated for 50 s with EGF and then fixed before permeabilization (a). Cells were counterstained with rhodamine-phalloidin to localize F-actin (b). Cofilin is localized close to the membrane at the leading edge along with F-actin.
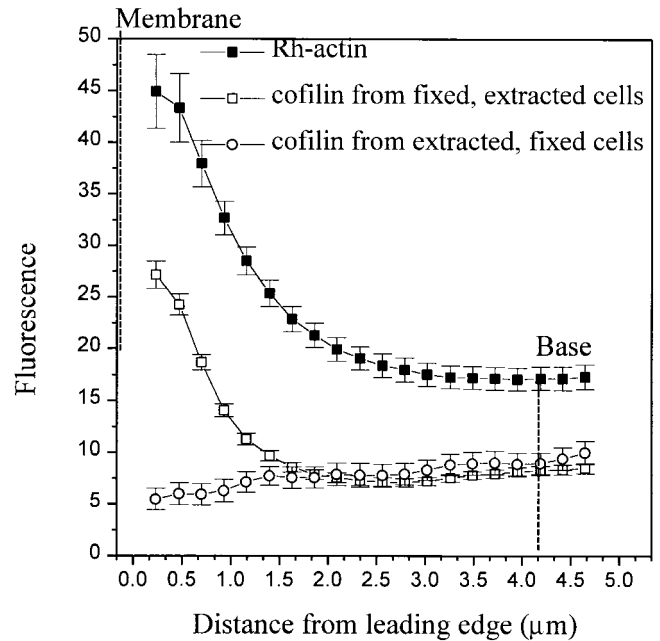
mixture of formaldehyde and glutaraldehyde for 1 h before detergent extraction (Bamburg and Bray, 1987). Although this prevented the localization of cofilin and barbed ends in the same cell, it permitted the localization of cofilin in cells at various times after stimulation without the artefact of cofilin extraction. In resting MTLn3 cells, cofilin is distributed diffusely in the cytoplasm (Fig. 1 b). Upon EGF stimulation, cofilin is recruited to the leading edge (Fig. 1 d), colocalizing with F-actin (Fig. 2).

To compare the distribution of cofilin relative to free barbed ends, parallel cultures were prepared to detect free barbed ends using rhodamine-actin incorporation (Chan et al., 1998), and cofilin using anticofilin antibody (Ab287). Quantitative analysis of the distribution of cofilin and free barbed ends in lamellipods shows overlapping localization, i.e., both localize very close to the plasma membrane (Fig. 3). The percentage of total cellular cofilin present in the leading edge increases from 4% in resting cells to 8% after EGF stimulation. In kinetic studies (Fig. 4), localization of cofilin to the leading edge peaks at 50 s after EGF stimulation, corresponding with the peak of barbed end appearance in the leading edge after stimulation. Concomitantly, accumulation of F-actin in the leading edge reaches a maximum by 60 s after stimulation (Chan et al., 1998).
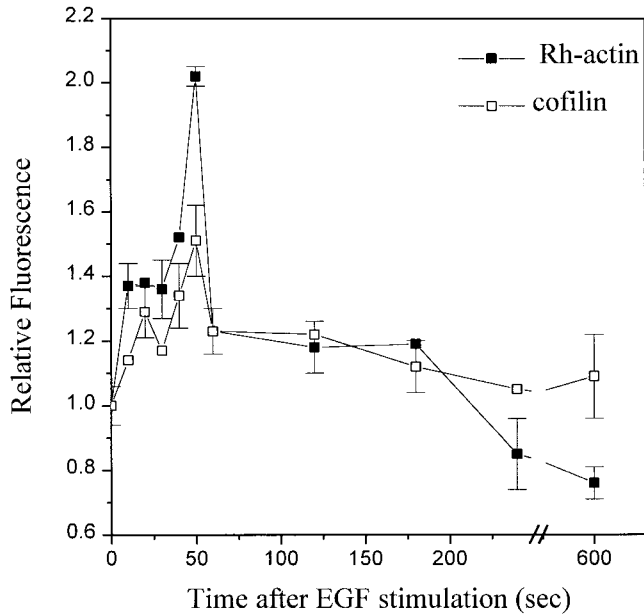
Figure 4. Cofilin and barbed ends appear in the leading edge at the same time after stimulation. Cofilin (open squares) in the leading edge is maximal at 50 s after stimulation, a time which is identical to the peak of appearance of free barbed ends (filled squares). Error bars are SEM. $n = 20$ cells.

Figure 5. EGF stimulates an increase in the number of pointed ends in cells. MTLn3 cells were stimulated with EGF, lysed, centrifuged, and the amount of DNase I bound to actin filaments was determined as described in Materials and Methods. The number of filament pointed ends was calculated as described in Materials and Methods. The number of filaments increases transiently after EGF stimulation by 60,000. Error bars are SEM. $n = 3$–4 experiments.

Quantitation and Localization of Free Pointed Ends

The results of immunofluorescence and kinetic studies shown here, combined with previous reports showing that cofilin can increase the number of free barbed ends in vitro (Du and Freiden, 1998; Maciver et al., 1998; Ichetovkin et al., 1999), suggest that cofilin could be associated with the production of free barbed ends as they appear after EGF stimulation. If cofilin-mediated severing of preexisting actin filaments occurs transiently and locally at the leading edge after EGF stimulation, free barbed and pointed ends would be exposed and the number of actin filaments should increase in the leading edge. We investigated this possibility by quantitating the number of pointed ends of actin filaments in low-speed Triton-insoluble cytoskeletons using a DNase I binding assay. DNase I binds the pointed ends of actin filaments with high affinity, and can thus be used to quantify directly the number of pointed ends in cells (Podolski and Steck, 1990; Eddy et al., 1997). As shown in Fig. 5, the number of filaments quantitated in low-speed Triton-insoluble cytoskeletons increases by 1.5-fold, which corresponds to a net increase of 6×10^4 pointed ends per cell within 50 s after EGF stimulation.

To identify where these new pointed ends are localized during stimulation, we bound DNase I to saponin-permeabilized cells, then immunostained for incorporation of exogenous DNase I with anti–DNase I IgG. As shown in Fig. 6 A, in resting cells DNase I localizes to DNA in the nucleus and to actin filaments in stress fibers (Fig. 6 A, arrow) as well as in the cell cortex. After EGF stimulation, the DNase I staining pattern is identical to that in the resting cells, except that the filaments in the cell cortex (Fig. 6
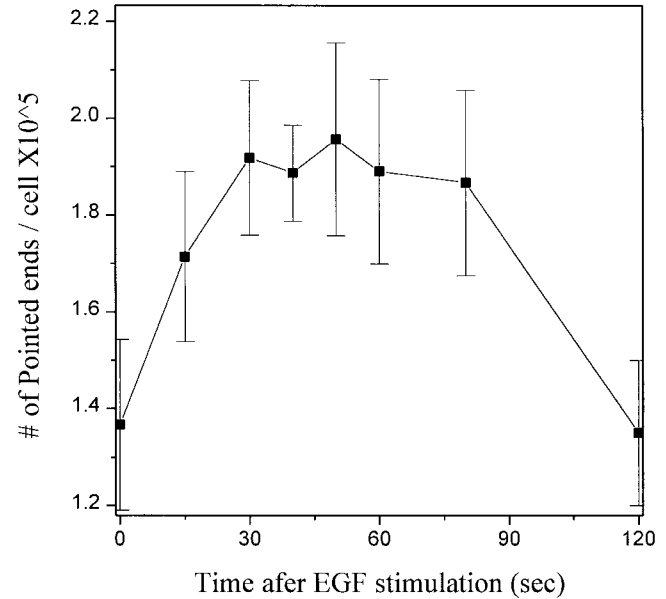
A, arrowheads) are stained at much higher intensity, indicating an increase in the number of pointed ends near the plasma membrane. Fig. 6 B shows the leading edge of cells like those in Fig. 6 A at higher magnification, clearly demonstrating the increase of pointed end staining at the leading edge (Fig. 6 B, arrowhead) of EGF-stimulated cells (EGF 50 sec) compared with that of resting cells (EGF 0).

Quantitation of the DNase I binding by measuring pixel intensity (Fig. 7) demonstrates a 1.5-fold increase in the number of pointed ends at the leading edge compartment, but not in stress fibers, after EGF stimulation. In control experiments, where DNase I binding to the pointed end of F-actin was blocked by pretreatment with equal molar amounts of G-actin, cytoplasmic binding sites for DNase I are blocked, indicating that DNase I is binding to the pointed ends of actin filaments in the cytoplasm (Fig. 7, inset). These results are consistent with our previously reported twofold increase after EGF stimulation in pointed end incorporation of 2 µM rhodamine-actin at the leading edge in gelsolin-capped cytoskeletons (Chan et al., 1998). They are also consistent with the 1.5-fold increase in filament density measured after stimulation at the leading edge using EM (Bailly et al., 1999). The fact that a 1.5–2-fold increase in pointed ends at the leading edge of stimulated cells is measured using three different methods (Chan et al., 1998; Bailly et al., 1999) (Figs. 5 and 7) indicates that the number of DNase I molecules bound is a direct measurement of the number of filaments present in the cytoplasm. These results also indicate that the number of filaments is increasing at the leading edge after stimulation.
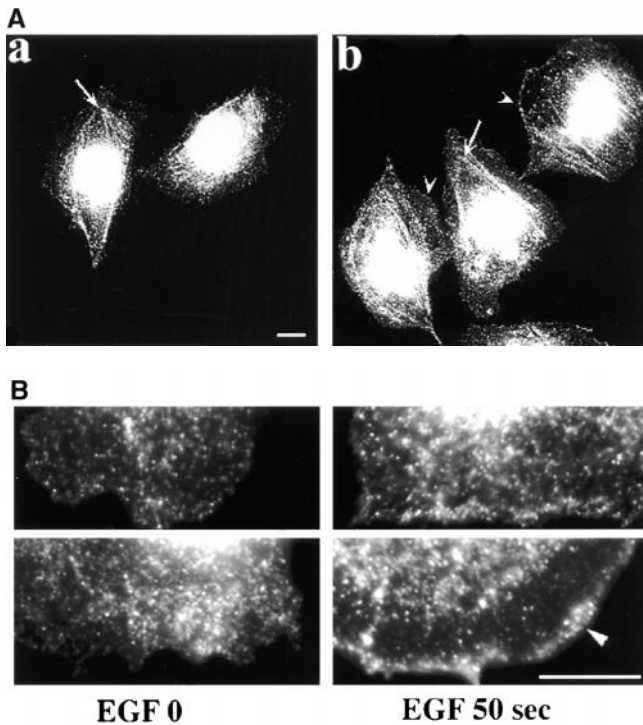
Figure 6. EGF stimulates the appearance of pointed ends at the leading edge. The binding of exogenous DNase I to permeabilized cells was detected by immunofluorescence with anti–DNase I to localize pointed ends. (A) In unstimulated cells (panel a), pointed ends are present mostly in the stress fibers (arrow) and scattered throughout the cytoplasm including the cell cortex. Upon stimulation with EGF for 50 s (b), pointed ends are present in stress fibers, and like barbed ends, increase in the leading edge (arrowhead). (B) EGF-stimulated cells (EGF 50 sec) have intense DNase I incorporation at the leading edge (arrowhead) compared with that of unstimulated cells. Bar, 10 μm.

Evidence for Cofilin Severing Activity in MTLn3 Cells

To determine if severing could contribute to the increase in filament number, a light microscope severing assay was used to determine if a cofilin-mediated severing activity is turned on during EGF stimulation of MTLn3 cells. This assay allows the experimenter to visualize the cutting of filaments directly in the light microscope using fluorescent F-actin. As shown in Fig. 8 A, only a small amount of filament severing is observed when filaments are perfused with cell lysates prepared from resting cells. However, when filaments are perfused with cell lysate from EGF-stimulated cells, severing activity is increased dramatically.

To identify the type of severing protein involved in this stimulated severing activity, we took advantage of a difference between the severing activities of the gelsolin and cofilin families of severing proteins. Phalloidin inhibits severing of cofilin-like proteins by competing with cofilin for binding to actin filaments, but does not block the severing activity of gelsolin-like proteins. We confirmed this by measuring severing of phalloidin-saturated filaments with either gelsolin or cofilin. Only gelsolin severed filaments under these conditions (data not shown). Next, we measured the ability of the severing activity in cell extracts to sever phalloidin-saturated F-actin. As shown in Fig. 8 A,
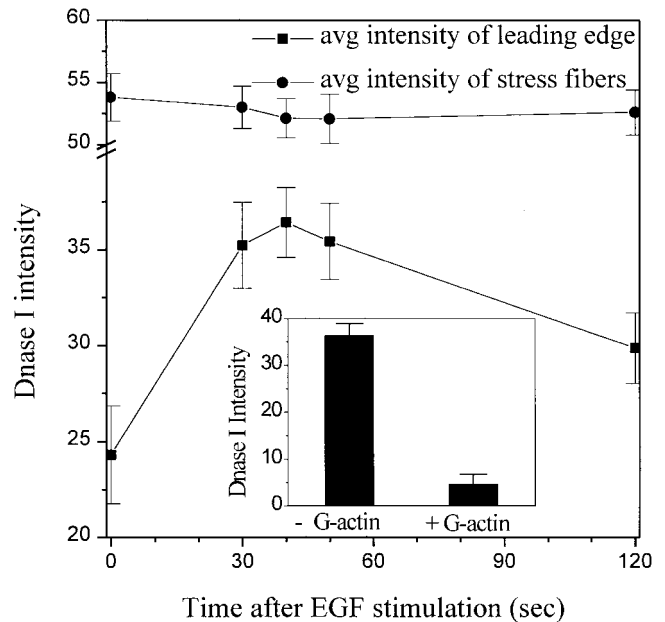
Figure 7. Kinetics of pointed end appearance after EGF stimulation. Pointed ends increase in the leading edge (filled squares) but remain constant in stress fibers (filled circles) after EGF stimulation. Pretreatment of DNase 1 with equal molar amounts of G-actin (inset) blocks pointed end detection at the leading edge indicating specificity of DNase I for pointed ends in situ. Error bars are SEM. $n = 30$ cells.

saturation of actin filaments with phalloidin inhibits the severing activity present in extracts from stimulated cells, indicating that a cofilin-mediated severing reaction operates in the EGF-stimulated cells. The severing activity present in MTLn3 cell lysates was 1.3-fold in resting lysates compared with buffer, and increased to 1.9-fold in lysates from EGF-stimulated cells (Fig. 8 B). The EGF-stimulated severing activity decreases to background levels when the actin filaments are saturated with phalloidin.

To investigate if the severing activity in cell lysates is specifically due to cofilin, we characterized a monospecific polyclonal antibody (Ab286) that was designed to recognize the actin binding site on cofilin (amino acids 104–117) and block cofilin's severing activity. Affinity purified Ab286 was added to purified rat recombinant cofilin and cofilin's severing activity in the light microscope assay was compared with that in the presence of nonimmune IgG. As shown in Fig. 9 A, addition of a molar excess (30:1) of affinity purified Ab286, but not nonimmune IgG, to purified recombinant rat cofilin inhibits its severing activity.

Ab286 was then used as a function-blocking antibody to inhibit cofilin's severing activity in cell extracts. As shown in Fig. 9 B, addition of Ab286 (but not nonimmune IgG) to cell extracts completely inhibited severing activity in extracts from both resting and stimulated cells. Therefore, cofilin is responsible for the severing activity detected in resting and stimulated cell lysates.

Microinjection of Function-blocking Antibodies Against Cofilin Inhibits EGF-stimulated Lamellipod Extension and Barbed End Appearance

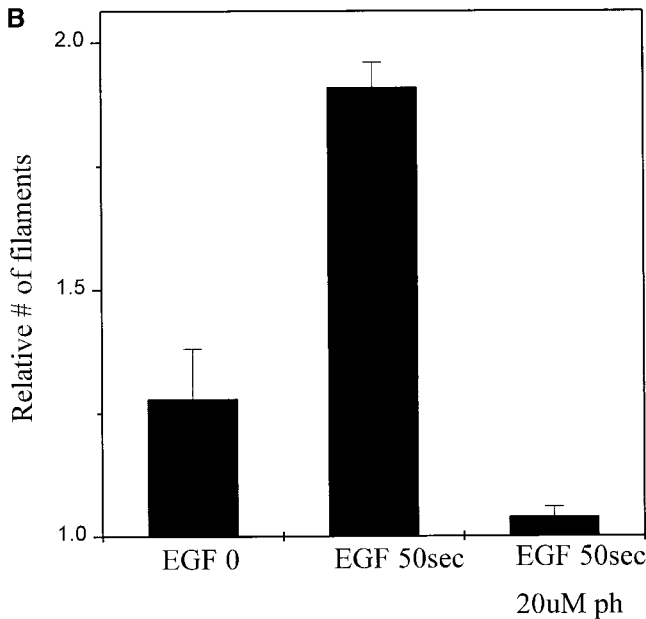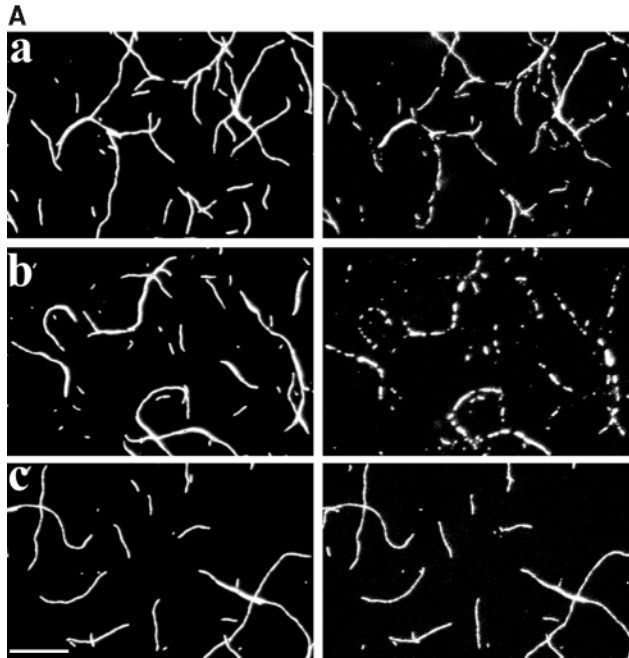To investigate the function of cofilin in vivo, antibody

A

B

Figure 8. EGF stimulates a phalloidin-sensitive severing activity in MTLn3 cell lysates. (A) Cells were either untreated (panel a) or treated with EGF for 50 s (panels b and c), lysed, and the lysate was perfused into a chamber containing F-actin (panels a and b) or phalloidin-saturated F-actin (panel c). All images shown are 30 s (left panels) and 20 min (right panels) after perfusion. Severing activity increases dramatically in cell lysates from EGF-stimulated cells (panel b), compared with unstimulated cells (panel a). The EGF-stimulated severing activity is not observed with phalloidin-saturated actin filaments (panel c). (B) Quantitation of the phalloidin-sensitive EGF-stimulated severing activity. Severing activity in MTLn3 cell lysates increases from 1.3-fold relative to buffer to 1.9-fold after EGF stimulation. The EGF-stimulated severing activity decreases to 1.04-fold relative to buffer with phalloidin-saturated actin filaments. The number of filaments in the same field were counted 30 s and 20 min after perfusion. The relative number of filaments was calculated as the ratio of the number of filaments at 20 min divided by the number of filaments 30 s after perfusion. Error bars are SEM. $n = 3$ experiments.
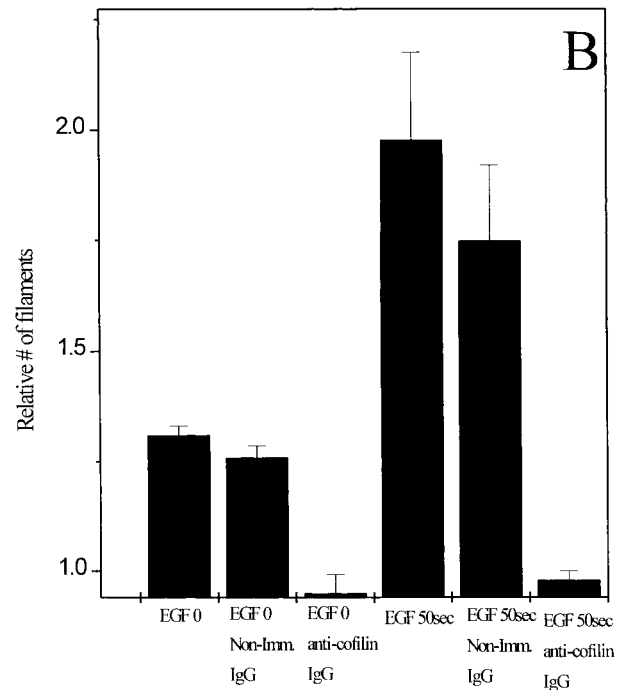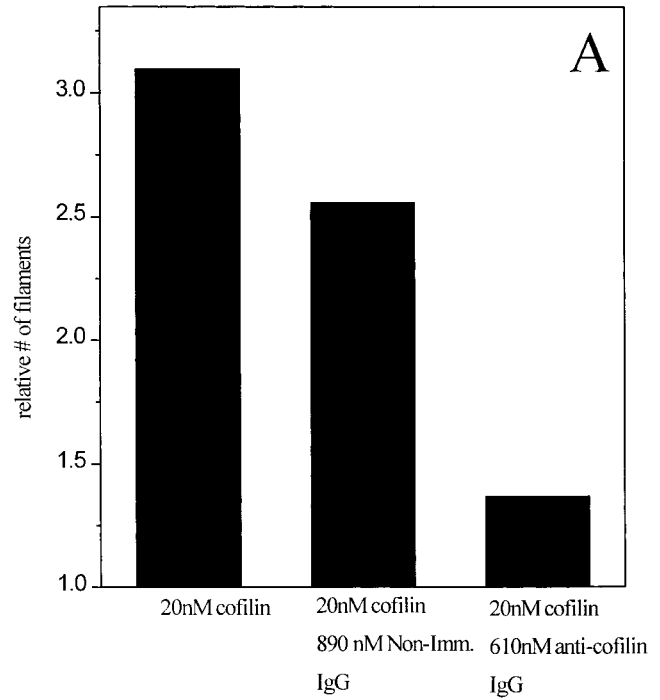

Figure 9. EGF stimulates cofilin's severing activity in MTLn3 cell lysates. (A) 20 nM purified rat cofilin was incubated with either 610 nM anticofilin (Ab286) or 890 nM nonimmune IgG in lysis buffer for 1 h and then perfused into a chamber containing F-actin. Anticofilin Ab286 but not noimmune IgG inhibits the severing activity of purified rat cofilin. (B) MTLn3 cell lysates from resting and stimulated cells were incubated with either 610 nM anticofilin (Ab286) or 890 nM nonimmune IgG in lysis buffer for 1 h and then perfused into a chamber containing F-actin. Severing activities in both resting and stimulated cell lysates were inhibited with anticofilin (Ab286)-treated cell lysates, an effect not observed in nonimmune IgG treated cell lysates. Error bars show SEM. $n = 3$ experiments.

	Control IgG	Ab286
Number of experiments	4	6
Total noninjected cells	347	536
Total injected cells	260	385
Ratio cell area injected/noninjected*	0.97 ± 0.03	1.02 ± 0.04
Ratio mean intensity of F-actin injected/noninjected*	1.09 ± 0.01	1.12 ± 0.02

Area and F-actin content were quantified using NIH Image on images as described in Materials and Methods. Both control nonimmune rabbit IgG and Ab286 anticofilin were microinjected at a concentration of 6 mg/ml. 1–2 h after microinjection, the cells were stimulated for 1 min with EGF and fixed and stained for F-actin.

*For each parameter (area and mean intensity) measured, the values obtained for the microinjected cells were ratioed to the values obtained for the noninjected cells in the same field to account for any intercoverslip differences. Mean ± SEM.

Figure 10. Microinjection of function-blocking antibodies against cofilin inhibits lamellipod extension after EGF stimulation. Cells were microinjected with function-blocking Ab286, or nonimmune rabbit IgG at 6 mg/ml, and their protrusive response to stimulation by EGF was analyzed 1–2 h later. Diamonds, control cells that have not been injected; squares, cells injected with nonimmune IgG; and circles, cells microinjected with Ab286. Results are the mean of seven (total 75 cells) and four (total 25 cells) experiments for the nonimmune IgG and Ab286, respectively. Control cells (total 73) were noninjected cells from the 7 experiments done with the nonimmune IgG. SEM < 1% for each curve.

Ab286, which inhibits the severing activity of pure recombinant cofilin as well as cofilin in cell extracts (see above), was microinjected into MTLn3 cells. Microinjection of these function-blocking antibodies against cofilin did not alter cell morphology for at least up to 2 h after injection (in particular, cell spreading as evaluated by area measurements was unaffected [Table I]). However, the ability of cells to extend lamellipods after EGF stimulation was strongly inhibited (Fig. 10). On the other hand, control cells injected with comparable amounts of nonimmune rabbit IgG extended lamellipods after stimulation with EGF with the expected kinetics and amplitude (Segall et al., 1996; Bailly et al., 1998b).

The ability of function-blocking antibodies against cofilin to inhibit lamellipod extension suggests that cofilin activity is required for actin polymerization at the leading edge after EGF stimulation, since actin polymerization is known to be required for lamellipod extension. However, these results did not distinguish how cofilin is functioning to affect actin polymerization at the leading edge. Cofilin could affect polymerization either: (a) indirectly, by increasing the rate of filament turnover to supply monomers for polymerization (Carlier et al., 1997; Ressad et al., 1999; Svitkina and Borisy, 1999); or (b) directly, by severing filaments to generate new barbed ends used to nucleate actin polymerization (Du and Freiden, 1998; Maciver et al., 1998; Ichetovkin et al., 1999). To distinguish these possibilities, we measured the ability of cells microinjected with function-blocking antibodies against cofilin to mobilize barbed ends after EGF stimulation.

Free barbed ends can be localized and quantified directly in cells by light permeabilization in the presence of concentrations of labeled G-actin sufficient to polymerize onto barbed but not pointed ends (Symons and Mitchison, 1991; Chan et al., 1998; Bailly et al., 1999). We have shown previously that the kinetics of barbed end appearance after stimulation are tightly controlled, with a maximum at 50–60 s after stimulation with EGF (Fig. 4; Bailly et al., 1999). We thus analyzed barbed end distribution in cells microinjected with function-blocking Ab286 or control nonimmune IgG at peak stimulation (stimulation with EGF for 1 min). As shown in Fig. 11 B, cells microinjected with control antibodies did not display any alteration in the distribution of barbed ends after stimulation, with typ-
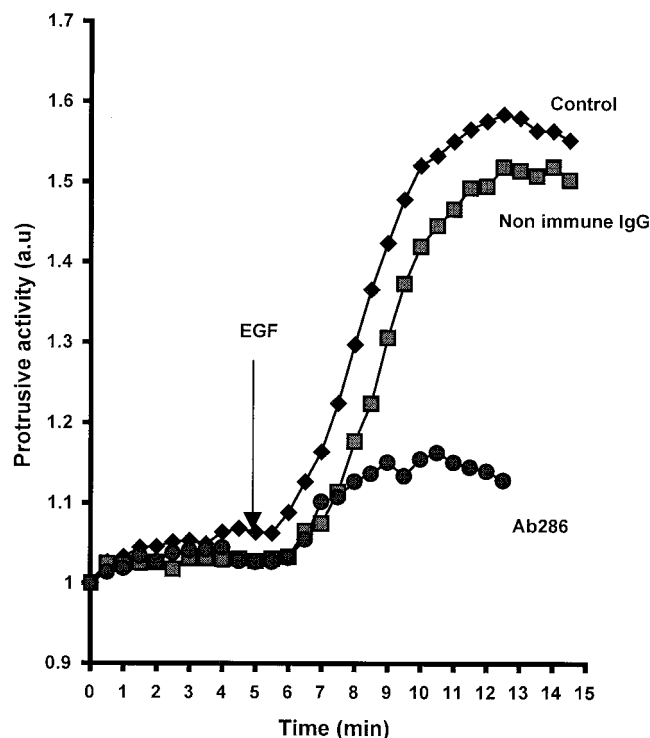
ical incorporation of labeled actin at the leading edge of the cells (Chan et al., 1998; Bailly et al., 1999). However, a large proportion of the cells injected with function-blocking antibodies against cofilin totally failed to generate barbed ends in the leading edge after EGF stimulation (Fig. 11, A and A′). Indeed, the proportion of cells that did not show any labeled actin incorporation at the leading edge after stimulation more than doubled in cells microinjected with the anticofilin compared with control cells injected with nonimmune IgG (Fig. 11 C). Moreover, this number is likely to be an underestimate of the inhibition, since only cells with complete inhibition of barbed ends at the leading edge (typical examples shown in Fig. 11, A and A′) were scored in this assay, whereas cells with partial decreases in barbed end intensity were not included.

Finally, to determine if the failure of cells microinjected with Ab286 to generate barbed ends was due to the inhibition of cofilin's severing activity, and not simply the consequence of a shortage of actin monomers due to the blocking of actin turnover by cofilin, we evaluated the amounts of F-actin present in the microinjected cells at the time barbed ends were measured (1 min after EGF stimulation). The amount of F-actin in cells microinjected with
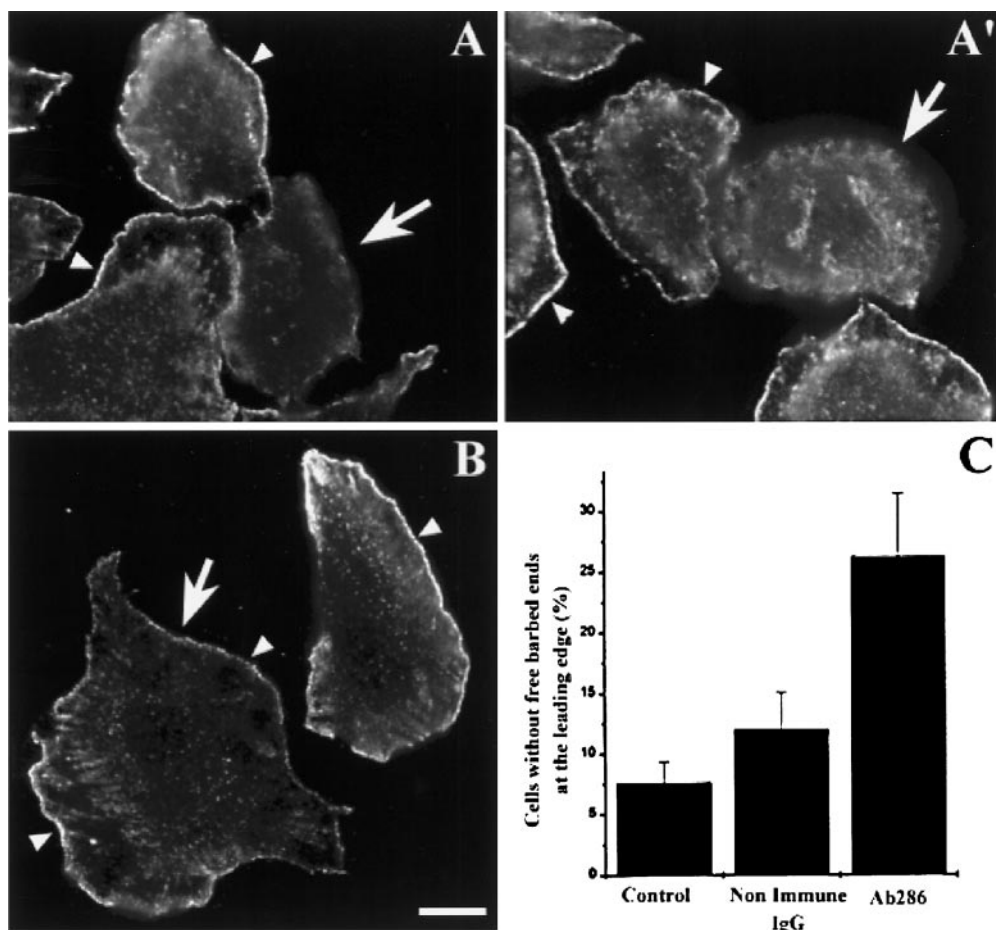
Figure 11. Microinjection of function-blocking antibodies against cofilin inhibits the appearance of free barbed ends after EGF stimulation. Cells were microinjected with 6 mg/ml of either function-blocking Ab286 (A and A′) or nonimmune IgG (B), and processed for barbed end localization 1–2 h after microinjection as described in Materials and Methods. Microinjected cells are indicated with arrows. Arrowheads indicate the typical (circumferential) incorporation of labeled actin at the leading edges visualizing the free barbed ends generated after EGF stimulation. Free barbed ends are present in control cells in all three panels as well as in cell microinjected with nonimmune IgG (B), but absent in cells injected with Ab286 (A and A′). Bar, 10 μm. (C) Quantification of the proportion of cells that failed to generate the typical pattern of barbed ends at the leading edge (as shown in A and A′). Results (mean ± SEM) are from a total of 398 cells (14 experiments) for Ab286, 118 cells (4 experiments) for nonimmune IgG, and 1,213 cells for the noninjected control cells in the same microscope fields.

anticofilin was quantified by pixel intensity after staining with rhodamine-labeled phalloidin, and compared with control cells either not injected or injected with control IgG. We found that 1–2 h after microinjection, there is no significant increase in the amount of F-actin in cells injected with cofilin antibodies compared with control cells (Table I). This indicates that the concentration of actin monomers in vivo was unlikely to be significantly affected by microinjection of blocking antibodies against cofilin for the brief period used in these experiments.

Discussion

Our study provides a detailed analysis in vivo and in vitro of the role of cofilin in EGF-stimulated lamellipod extension and actin polymerization. We have demonstrated that: (a) cofilin is recruited to the leading edge at the same time and in the same location as free barbed ends in response to stimulation with EGF; (b) stimulation with EGF results in an increase in the number of filaments (Chan et al., 1998; Bailly et al., 1999; this study), as well as a decrease in filament length at the leading edge (Bailly et al., 1999); (c)

EGF stimulates cofilin's severing activity in cell lysates; and (d) function-blocking antibodies against cofilin suppress the appearance of free barbed ends and lamellipod protrusion after stimulation with EGF.

Altogether, these results directly implicate cofilin in the dynamics of actin polymerization at the leading edge of cells after stimulation with EGF. They also indicate that cofilin's severing activity is likely to play a direct role in the mobilization of free barbed ends at the leading edge after stimulation.

Cofilin Is Recruited to the Leading Edge during Barbed End Mobilization

The results shown here demonstrate that cofilin is recruited to the leading edge of the lamellipod, where barbed ends appear after EGF stimulation. However, we have also found, as previously reported for other types of cells (Bamburg and Bray, 1987), that the visualization of cofilin in the leading edge is highly sensitive to detergent extraction. The ease with which cofilin is extracted from cells even during light permeabilization before fixation

suggests that cofilin might be only transiently associated with the actin cytoskeleton in situ. This is consistent with the biochemical properties of cofilin in vitro, where purified cofilin bound to F-actin is released upon stimulation of cofilin's severing and depolymerizing activities (Hayden et al., 1993). Our results support this conclusion, since the EGF-stimulated recruitment of cofilin that we observed at the leading edge is only transient and cotemporal with barbed end appearance. They also suggest that transient activation of cofilin plays a role in the mobilization of barbed ends and their polymerization at the leading edge.

The localization of cofilin at the extreme leading edge of extending lamellipods shown here is inconsistent with previous elegant studies in *Xenopus* keratocytes, where cofilin was localized starting ~1 μm back from the edge (Svitkina and Borisy, 1999). However, as described before (Bailly et al., 1999), the ultrastructure of the cytoskeleton at the leading edge in MTLn3 cells is quite distinct from that of keratocytes, and more comparable to the general organization of the cytoskeleton reported for mammalian fibroblasts and chemotactic ameboid cells such as macrophages and leukocytes (Ryder et al., 1984; Hartwig and Shevlin, 1986). Furthermore, when cofilin was localized in the lamellipods of fibroblasts in parallel with keratocytes (Svitkina and Borisy, 1999), it was found to be distributed at the extreme leading edge of the lamellipod of fibroblasts, a pattern comparable to that described here in MTLn3 cells. Finally, the precise location of free barbed ends has not been determined in keratocytes as done for MTLn3 cells (Bailly et al., 1999) and fibroblasts (Symons and Mitchison, 1991), making the relative locations of cofilin and free barbed ends uncertain in keratocytes.

Altogether, these results suggest that the precise localization of cofilin at the leading edge may vary depending on cell type and the type of motility being exhibited. For example, keratocytes exhibit the continuous extension of the leading edge without cycles of extension and retraction as seen in fibroblasts and MTLn3 cells. In addition, F-actin in keratocytes does not exhibit the characteristic centripetal flow relative to the substratum at the leading edge seen in fibroblasts (Theriot and Mitchison, 1992), suggesting differences between fibroblasts and keratocytes in the dynamics and anchoring of the F-actin network at the leading edge (Smilenov et al., 1999). Since the relative retention of cofilin in extracted cells may depend on the relative rate of turnover of the filaments at the leading edge, it is possible that variations in the localization of cofilin in the leading edge occur among the different cell types due to differences in actin dynamics.

EGF Stimulation Increases the Number of Actin Filaments at the Leading Edge

To identify the mechanisms responsible for the generation of free barbed ends at the leading edge, we determined the number of filaments in the leading edge relative to the whole cell. We found that the number of filaments increases by 1.5-fold, an increase of 60,000 filaments per cell, within 50 s after EGF stimulation. In situ localization of pointed ends using DNase I staining demonstrates that the increase in the number of filaments is confined to the leading edge and does not occur within stress fibers or in the

general cytoplasm. These results are consistent with previous indirect measurements of actin filament number in cells after EGF stimulation, using the incorporation of 2 μM rhodamine-actin to detect the number of pointed ends in cytoskeletons capped with gelsolin–actin complex (Chan et al., 1998), as well as the direct measurement of filament density at the leading edge using quantitative EM (Bailly et al., 1999). Thus, these three different assays for measuring actin filament numbers agree that the number of filaments increases significantly after EGF stimulation, and that the increase in filament number occurs specifically in the leading edge.

The increase in filament number at the same time and place as the increase in free barbed ends after stimulation is inconsistent with a pure uncapping mechanism. In a pure uncapping mechanism, filament length would increase as a result of polymerization from free barbed ends, but the number of filaments before and after EGF stimulation would remain constant. However, an increase in filament number alone does not distinguish between severing and de novo nucleation as the dominant mechanism responsible for the increase in free barbed ends at the leading edge in MTLn3 cells.

EGF Stimulates Cofilin Severing Activity

To determine if cofilin's severing activity is turned on by EGF stimulation, we used a light microscope severing assay to directly visualize filament severing activity in lysates from resting and stimulated MTLn3 cells. Results from the light microscope severing assay show that cofilin's severing activity is turned on by the stimulation of cells with EGF. These results in cell lysates are consistent with the EGF-induced decrease in filament length, with the specific loss of long filaments, observed in the electron microscope in cells at the leading edge as reported previously (Bailly et al., 1999). Together, these results predict that cofilin-mediated severing activity is present at the leading edge after stimulation with EGF.

Function-blocking Antibodies and the Role of Cofilin In Vivo

The light microscope assay used to investigate the severing activity of cofilin in cell lysates was also useful in demonstrating the function-blocking activity of Ab286 toward cofilin's severing activity. Microinjection of these antibodies into cells inhibited the EGF-stimulated extension of lamellipods, supporting a role for cofilin in the turnover of actin filaments at the leading edge to supply a monomer for new assembly as proposed elsewhere (Carlier et al., 1997; Loisel et al., 1999; Ressad et al., 1999; Svitkina and Borisy, 1999).

However, the direct involvement of cofilin in generating barbed ends after stimulation is supported by the finding that cells microinjected with anticofilin were inhibited in their ability to generate new barbed ends at the leading edge after stimulation with EGF. The amounts of G- (77 μM) and F-actin (76 μM) in MTLn3 cells are known (Edmonds et al., 1996). Since the amount of F-actin in cells was not changed within 2 h of microinjection of anticofilin, the failure of cells to generate free barbed ends was unlikely to be due to depletion of G-actin in vivo after the in-

hibition of cofilin. Furthermore, since the G-actin used to visualize free barbed ends in the assay described here was supplied exogenously, any activated nucleation template that was made before permeabilization would incorporate the exogenous G-actin and be detected regardless of whether there was enough endogenous G-actin in the cells to support polymerization. Therefore, the inhibition of lamellipod extension by function-blocking antibodies against cofilin is consistent with a more direct involvement of cofilin in barbed end mobilization, since the polymerization of free barbed ends is believed to supply the force for protrusion of the leading edge (Condeelis, 1993).

How Does Cofilin Contribute to the Appearance of Barbed Ends at the Leading Edge?

The results presented in this study demonstrate for the first time that cofilin's severing activity is turned on during stimulated lamellipod extension and that cofilin activity is required for the appearance of barbed ends. Cofilin could contribute to barbed end formation by two different mechanisms. The first mechanism, which has received a lot of attention recently in the literature, proposes that cofilin enhances indirectly the nucleation activity of the Arp2/3 complex by supplying actin monomers through its depolymerizing activity (Egile et al., 1999; Loisel et al., 1999; Ressad et al., 1999; Svitkina and Borisy, 1999). The second mechanism, based on biochemical studies (Bamburg, 1999; Du and Freiden, 1998; Maciver et al., 1998; Ichetovkin et al., 2000), proposes that cofilin can directly contribute barbed ends by severing actin filaments (Bailly et al., 1999).

The first mechanism is consistent with the known biochemical activities of Arp2/3 (Mullins et al., 1998; Machesky et al., 1999; Welch, 1999) and its location at the leading edge (Bailly et al., 1999; Svitkina and Borisy, 1999). However, it is inconsistent with the inhibition of barbed ends by anticofilin in the presence of either endogenous levels of G-actin or exogenous polymerization-competent G-actin sufficient for polymerization as discussed above. In addition, it is difficult to reconcile with the fact that polymerization-competent G-actin is present in vivo at concentrations exceeding 75 μM in MTLn3 cells before the stimulation of protrusion and motility. The second mechanism is consistent with increases in cofilin's severing activity and transient recruitment to the leading edge after stimulation. However, it is inconsistent with the rapid depolymerization of filaments in the presence of cofilin (Carlier et al., 1997). The synergistic interaction between cofilin and Arp2/3, where Arp2/3 caps and stabilizes short filaments produced by cofilin severing activity, may resolve the inconsistencies inherent in the above two mechanisms (Bailly et al., 1999). Further work will be required to measure the relative contributions of cofilin and Arp2/3 to the bursts of actin nucleation observed at the leading edge in response to chemotactic stimulation.

References

Abercrombie, M., J.E. Heaysman, and S.M. Pegrum. 1970. The locomotion of fibroblasts in culture. I. Movements of the leading edge. *Exp. Cell Res.* 59:393–398.

Aizawa, H., K. Sutoh, S. Tsubui, S. Kawashima, A. Ishii, and I. Yahara. 1995. Identification, characterization, and intracellular distribution of cofilin in *Dictyostelium discoideum. J. Biol. Chem.* 270:10923–10932.

Bailly, M., J.S. Condeelis, and J.E. Segall. 1998a. Chemoattractant-induced lamellipod extension. *Microsc. Res. Tech.* 43:433–443.

Bailly, M., L. Yan, G.M. Whitesides, J.S. Condeelis, and J.E. Segall. 1998b. Regulation of protrusion shape and adhesion to the susbtratum during chemotactic responses of mammalian carcinoma cells. *Exp. Cell Res.* 241:285–299.

Bailly, M., F. Macaluso, M. Cammer, A.Y. Chan, J. Segall, and J.S. Condeelis. 1999. Relationship between Arp2/3 complex and the barbed ends of actin filaments at the leading edge of carcinoma cells after epidermal growth factor stimulation. *J. Cell Biol.* 145:331–345.

Bamburg, J.R. 1999. Proteins of the ADF/cofilin family: essential regulators of actin dynamics. *Annu. Rev. Cell Dev. Biol.* 15:185–230.

Bamburg, J.R., and D. Bray. 1987. Distribution and cellular localization of actin depolymerizing factor. *J. Cell Biol.* 105:2817–2825.

Bamburg, J.R., A. McGough, and S. Ono. 1999. Putting a new twist on actin: ADF/cofilins modulate actin dynamics. *Trends Cell Biol.* 9:364–370.

Carlier, M., V. Laurent, J. Santolini, R. Melki, D. Didry, G.-X. Xia, Y. Hong, N.-H. Chua, and D. Pantaloni. 1997. ADF/cofilin enhances the rate of filament turnover: implication in actin-based motility. *J. Cell Biol.* 136:1307–1323.

Chan, A.Y., S. Raft, M. Bailly, J.B. Wyckoff, J.E. Segall, and J.S. Condeelis. 1998. EGF stimulates an increase in actin nucleation and filament number at the leading edge of the lamellipod in mammary adenocarcinoma cells. *J. Cell Sci.* 111:199–211.

Chen, P., K. Gupta, and A. Wells. 1994. Cell movement elicited by epidermal growth factor receptor requires kinase and autophosphorylation but is separable from mitogenesis. *J. Cell Biol.* 124:547–555.

Condeelis, J. 1993. Life at the leading edge: the formation of cell protrusions. *Annu. Rev. Cell Biol.* 9:411–444.

Condeelis, J. 1998. The biochemistry of animal cell crawling. *In* Motion Analysis of Living Cells. D. Soll, editor. Wiley-Liss, Inc., New York. 85–100.

Djafarzadeh, S., and V. Niggli. 1997. Signaling pathways involved in dephosphorylation and localization of the actin-binding protein cofilin in stimulated human neutrophils. *Exp. Cell Res.* 236:427–435.

Du, J., and C. Freiden. 1998. Kinetic studies on the effect of yeast cofilin on yeast actin polymerization. *Biochemistry.* 37:13276–13284.

Eddy, R.J., J. Han, and J.S. Condeelis. 1997. Capping protein terminates but does not initiate chemoattractant-induced actin assembly in *Dictyostelium. J. Cell Biol.* 139:1243–1253.

Egile, C., T. Loisel, V. Laurent, R. Li, D. Pantaloni, P. Sansonetti, and M. Carlier. 1999. Activation of the CDC42 effector N-WASP by the *Shigella flexneri* IcsA protein promotes actin nucleation by Arp2/3 complex and bacterial actin-based motility. *J. Cell Biol.* 146:1319–1332.

Edmonds, B.T., J. Wyckoff, Y.G. Yeung, Y. Wang, E.R. Stanley, J. Jones, J. Segall, and J. Condeelis. 1996. Elongation factor-1α is an overexpressed actin binding protein in metastatic rat mammary adenocarcinoma. *J. Cell Sci.* 109:2705–2714.

Fedorov, A.A., P. Lappalainen, E.V. Fedorov, D.G. Drubin, and S.C. Almo. 1997. Structure determination of yeast cofilin. *Nat. Struct. Biol.* 4:366–369.

Handel, S.E., K.A.K. Hendry, and P. Sheterline. 1990. Microinjection of covalently cross-linked actin oligomers causes disruption of existing actin filament architecture in ptK2 cells. *J. Cell Sci.* 97:325–333.

Hartwig, J.H., and P. Shevlin. 1986. The architecture of actin filaments and the ultrastructural location of actin binding protein in the periphery of lung macrophages. *J. Cell Biol.* 103:407–425.

Hartwig, J.H., G.M. Bokoch, C.L. Carpenter, P.A. Janmey, L.A. Taylor, A. Toker, and T.P. Stossel. 1995. Thrombin receptor ligation and activated Rac uncap filament barbed ends through phosphoinositide synthesis in permeabilized platelets. *Cell.* 82:643–653.

Hayden, S.M., P.S. Miller, A. Brauweiler, and J.R. Bamburg. 1993. Analysis of the interactions of ADF with G and F-actin. *Biochemistry.* 32:9994–10004.

Heyworth, P.G., J.M. Robinson, J. Ding, B.A. Ellis, and J.A. Badwey. 1997. Cofilin undergoes rapid dephosphorylation in stimulated neutrophils and translocates to ruffled membranes enriched in products of the NADPH oxidase complex. Evidence for a novel cycle of phosphorylation and dephosphorylation. *Histochem. Cell Biol.* 108:221–233.

Ichetovkin, I., J. Han, K.M. Pang, D.A. Knecht, and J.S. Condeelis. 2000. Actin filaments are severed by both native and recombinant cofilins but to differ-

ent extents. *Cell Motil. Cytoskelet.* In press.

Knowles, G.C., and C.A.G. McCulloch. 1992. Simultaneous localization and quantification of relative G and F actin content: optimization of fluorescence labeling methods. *J. Histochem. Cytochem.* 40:1605–1612.

Lauffenburger, D.A., and A.F. Horwitz. 1996. Cell migration: a physically integrated molecular process. *Cell.* 84:359–369.

Loisel, T.P., R. Boujemaa, D. Pantaloni, and M.F. Carlier. 1999. Reconstruction of actin-based motility of *Listeria* and *Shigella* using pure proteins. *Nature.* 401:613–616.

Machesky, L.M., R.D. Mullins, H.N. Higgs, D.A. Kaiser, L. Blanchoin, R.C. May, M.E. Hall, and T.D. Pollard. 1999. Scar, a WASP-related protein, activates dendritic nucleation of actin filaments by the Arp2/3 complex. *Proc. Natl. Acad. Sci. USA.* 96:3739–3744.

Maciver, S.K., B.J. Pope, S. Whytock, and A.G. Weeds. 1998. The effect of two ADF/cofilins on actin filament turnover: pH sensitivity of F-actin binding by human ADF but not of *Acanthamoeba actophorin. Eur. J. Biochem.* 256: 388–397.

McGough, A., B. Pope, W. Chiu, and A. Weeds. 1997. Cofilin changes the twist of F-actin: implications for actin filament dynamics and cellular function. *J. Cell Biol.* 138:771–781.

Minaschek, J., J. Bereiter-Hahn, and G. Bertholdt. 1989. Quantitation of the volume of liquid injected into cells by means of pressure. *Exp. Cell Res.* 183: 434–442.

Mitchison, T.J., and L.P. Cramer. 1996. Actin-based cell motility and cell locomotion. *Cell.* 84:371–379.

Mullins, R.D., J.A. Heuser, and T.D. Pollard. 1998. The interaction of Arp2/3 complex with actin: nucleation, high affinity pointed end capping, and formation of branching networks of filaments. *Proc. Natl. Acad. Sci. USA.* 95: 6181–6186.

Podolski, J.L., and T.L. Steck. 1990. Length distribution of F-actin in *Dictyostelium discoideum. J. Biol. Chem.* 265:1312–1318.

Posnett, D.N., and J.P. Tam. 1989. Multiple antigenic peptide method for producing antipeptide site-specific antibodies. *Meth. Enzymol.* 178:739–746.

Posnett, D.N., H. McGrath, and J.P. Tam. 1988. A novel method for producing anti-peptide antibodies. Production of site-specific antibodies to the T cell antigen receptor beta-chain. *J. Biol. Chem.* 263:1719–1725.

Ressad, F., D. Didry, C. Egile, D. Pantaloni, and M.-F. Carlier. 1999. Control of actin filament length and turnover by actin depolymerizing factor (ADF/co-

filin) in the presence of capping proteins and Arp2/3 complex. *J. Biol. Chem.* 30:20970–20976.

Rohatgi, R., L. Ma, H. Miki, M. Lopez, T. Kirchhausen, T. Takenawa, and M.W. Kirschner. 1999. The interaction between N-WASP and the Arp2/3 complex links Cdc42-dependent signals to actin assembly. *Cell.* 97:221–231.

Ryder, M.I., R.N. Weinreb, and R. Niederman. 1984. The organization of actin filaments in human polymorphonuclear leukocytes. *Anat. Rec.* 209:7–20.

Segall, J.E., S. Tyerech, L. Boselli, S. Masseling, J. Helft, A. Chan, J. Jones, and J. Condeelis. 1996. EGF stimulates lamellipod extension in metastatic mammary adenocarcinoma cells by an actin-dependent mechanism. *Clin. Exp. Metastasis.* 14:61–72.

Smilenov, L., A. Mikhailov, R. Pelham, E. Marcantonio, and G. Gundersen. 1999. Focal adhesion motility revealed in stationary fibroblasts. *Science.* 286: 1172–1174.

Suzuki, K., T. Yamaguchi, T. Tanaka, T. Kawanishi, K. Nishimaki-Mogami, T. Yamamoto, T. Tsuji, T. Irimura, T. Hayakawa, and A. Takahashi. 1995. Activation induces dephosphorylation of cofilin and its translocation to plasma membranes in neutrophil-like differentiated HL-60 cells. *J. Biol. Chem.* 270: 19551–19556.

Svitkina, T.M., and G.G. Borisy. 1999. Arp2/3 complex and actin depolymerizing factor/cofilin in dendritic organization and treadmilling of actin filament array in lamellipodia. *J. Cell Biol.* 145:1009–1026.

Symons, M.H., and T.J. Mitchison. 1991. Control of actin polymerization in live and permeabilized fibroblasts. *J. Cell Biol.* 114:503–513.

Theriot, J., and T. Mitchison. 1992. Comparison of actin and cell surface dynamics in motile fibroblasts. *J. Cell Biol.* 118:367–377.

Verschueren, H., J. Dewit, J. De Braekeleer, V. Schirrmacher, and P. De Baetselier. 1994. Motility and invasive potency of murine T-lymphoma cells: effect of microtubule inhibitors. *Cell Biol. Int.* 18:11–19.

Welch, M.D. 1999. The world according to Arp: regulation of actin nucleation by the Arp2/3 complex. *Trends Cell Biol.* 9:423–427.

Xie, H., T. Turner, M.H. Wang, R.K. Singh, G.P. Siegal, and A. Wells. 1995. In vitro invasiveness of DU-145 human prostate carcinoma cells is modulated by EGF receptor-mediated signals. *Clin. Exp. Metastasis.* 13:407–419.

Yonezawa, N., Y. Homma, I. Yahara, H. Sakai, and E. Nishida. 1991. A short sequence responsible for both phosphoinositide binding and actin binding activities of cofilin. *J. Biol. Chem.* 266:17218–17221.